ELSEVIER

Materials Science and Engineering A226–228 (1997) 448–452

MATERIALS SCIENCE & ENGINEERING A

Bulk amorphous $Zn_{41}Sb_{59}$ and GaSb studied by neutron diffraction

U. Dahlborg [1,a,*], M. Calvo-Dahlborg[1] [a], A.I. Kolesnikov [b], O.I. Barkalov [b], V.E. Antonov [b], E.G. Ponyatovsky [b]

[a] *Department of Neutron Physics, Royal Institute of Technology, 100 44 Stockholm, Sweden*
[b] *Institute of Solid State Physics of the Russian Academy of Sciences, 142432 Chernogolovka, Moscow District, Russia*

Abstract

The structures of bulk amorphous $Zn_{41}Sb_{59}$ and of GaSb alloys, produced by solid state transformation of the high pressure crystalline phase, were studied by neutron diffraction. The results are compared with the structure of crystalline compounds of the same composition. The structure of the amorphous GaSb is interpreted in terms of a distorted network of ZnS blende type. The local atomic coordination in the ZnSb alloy is basically tetrahedral but the tetrahedra are deformed and interlinked. A comparison with the structure of other amorphous semiconducting materials with tetrahedral bonding is also presented. © 1997 Elsevier Science S.A.

Keywords: Bulk amorphous semiconductors; High pressure; $Zn_{41}Sb_{59}$; GaSb; Neutron diffraction

1. Introduction

Along with the traditional techniques for producing amorphous alloys based on deposition onto cold substrata or rapid quenching from the liquid state, a number of other techniques of amorphization, such as mechanical alloying, annealing of film multilayers, irradiation, etc. have been developed in recent years. These new methods are usually called solid state amorphization techniques. In spite of the fact that the processes are widely explored in industry, the mechanism behind this amorphization process is still not fully understood.

One of the solid state amorphization methods consists of a spontaneous amorphization of metastable phases (SAMP) [1]. The SAMP technique enables to obtain bulk amorphous samples of compositions very difficult or impossible to produce otherwise. The procedure of preparing the bulk amorphous alloys consists in the following sequence: (a) formation of new intermediate phase at a high pressure; (b) its rapid quenching under pressure down to liquid nitrogen temperature; (c) releasing pressure at low temperature; (d) heating at normal pressure. Until now the SAMP technique has been used to produce amorphous alloys, all semiconductors, of $Cd_{43}Sb_{57}$ [2], $Zn_{41}Sb_{59}$ [2], $Al_{32}Ge_{68}$ [3], $Ga_{50}Sb_{50}$ [2] and also $(GaSb)_{76}Ge_{24}$ [4]. Two of these alloys, $Zn_{41}Sb_{59}$ [5] and $Ga_{50}Sb_{50}$ [6], have been studied by neutron diffraction. Further investigations [7] have revealed that amorphous $Zn_{41}Sb_{59}$ produced by the SAMP technique corresponds to a metastable equilibrium state at ambient conditions. These results were recently theoretically interpreted and generalized [8]. It was specifically shown in the framework of a two-level model that amorphous states of the semiconducting compounds $A_{III}B_V$ with coordination number close to four are metastable phases at normal conditions and correspond to pronounced minima in the thermodynamic potential. Furthermore in the temperature–pressure-diagram calculated for these alloys at equiatomic concentration a line of first order phase transition exists from a low-pressure semiconducting amorphous phase to a high-pressure metallic amorphous phase.

However, it is also a debatable topic whether amorphous states of a material produced by different amorphization techniques generally have the same structure and whether these amorphous materials really are metastable phases or essentially non-equilibrium so-called 'frozen' states. This was recently elucidated from

* Corresponding author.
[1] Present address: LSG2M, CNRS UA 159, Ecole des Mines, Parc de Saurupt, 54042 Nancy Cedex, France.

PII S0921-5093(96)10662-6

a comparison of the structure of amorphous GaSb films, produced by the sputtering technique, and bulk amorphous GaSb, *a*-GaSb, produced by thermobaric quenching [6]. In the first case the structure was determined by X-ray and in the latter by neutron diffraction. The conclusion from this study was that the two structures are very similar but not identical.

We present below a comparative study of the results of a neutron diffraction investigation of bulk *a*-$Zn_{41}Sb_{59}$ [5] and *a*-GaSb [6] prepared by spontaneous amorphization of the high pressure crystalline phase. The comparison is made both on the level of the total structure factor *S(Q)* and of the calculated total pair distribution function, *g(r)*. The *S(Q)* is in the last section compared with the measured structure factors of *a*-silicon, *a*-germanium and *a*-carbon, available in the literature.

2. Experimental details

The neutron diffraction experiments were performed on the diffractometers LAD at the ISIS pulsed neutron source (Rutherford Appleton Laboratory, UK) and on SLAD at the R2 reactor at Studsvik (Sweden), respectively. The ISIS spallation neutron source produces a beam containing neutrons in a wide energy (and wavelength) range that gives the opportunity to measure the intensity of neutrons scattered from the sample as a function of time-of-flight at several different scattering angles simultaneously. Every measured spectrum can be directly transformed into a momentum transfer pattern and they are usually merged to give a final *S(Q)* of very good statistical accuracy. The LAD data are characterized by a wide range of neutron wavevector (momentum) transfers, $0.5 \leq Q \leq 30$ Å^{-1}. At the SLAD diffractometer, however, the wavelength of the incoming neutrons is fixed to 1.11 Å. The scattered neutrons were collected in an angular range from 6 to 140° yielding a range of momentum transfers from 0.5 to 10 Å^{-1}. The relevant scattering cross sections, given in Table 1, show that in the case of ZnSb the two kinds of atoms have almost the same coherent scattering cross section and they thus contribute with a similar weight to the measured total static structure factor *S(Q)*. For GaSb the contribution from the Ga nuclei dominates.

Table 1
Neutron scattering cross sections

Element	σ_{coh} (barns)	σ_{inc} (barns)
Zn	4.054	0.077
Ga	6.675	0.16
Sb	3.90	0.00

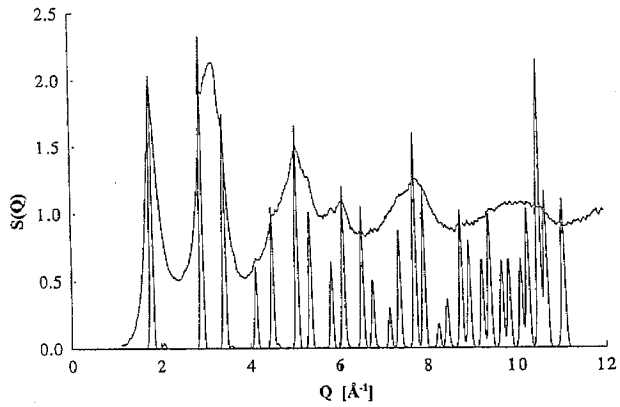

Fig. 1. Comparison of the structure factor *S(Q)* for amorphous GaSb at 100 K and the calculated diffraction pattern for the low pressure crystalline phase, GaSb-I.

The samples of *a*-$Zn_{41}Sb_{59}$ and *a*-GaSb consisted of a stack of cylindrical pellets packed in a vanadium can placed vertically in the neutron beam. Each pellet had a diameter of 7–8 mm and a height of about 2 mm.

3. Results

3.1. GaSb

Fig. 1 shows the static structure factor *S(Q)* for *a*-GaSb at 100 K obtained from the merging of the experimental diffraction patterns, measured at the different scattering angles on the LAD diffractometer. The *S(Q)* is characterized by rather sharp oscillations around 1.0 at *Q*-values up to 27.5 Å^{-1}. The positions and the full width at half maximum, FWHM, of the first two peaks of *S(Q)* are $Q_1 = 1.78$ Å^{-1}, $\Delta Q_1 = 0.33$ Å^{-1} and $Q_2 = 3.16$ Å^{-1}, $\Delta Q_2 = 0.60$ Å^{-1}.

The *S(Q)* curve in Fig. 1 exhibits several sharp features which could be interpreted as sample microcrystallinity or an indication of the existence of crystalline inclusions. However, from a careful analysis [6] it was concluded that the *a*-GaSb sample is really amorphous and not microcrystalline. If crystalline inclusions nevertheless were present in the sample, their abundance can be estimated to be less than 0.05% and their possible existence would consequently not influence the structure analysis.

The total pair distribution function $g(r) = G(r) + 1$, shown in Fig. 2, was obtained by Fourier transformation of *S(Q)* with $Q_{max} = 27.5$ Å^{-1}, using standard transformation techniques, including the use of a window function. *G(r)* is given by

$$G(r) = \frac{1}{2\pi^2 \rho_0 r} \int_0^{Q_{max}} Q[S(Q) - 1] \sin(Qr) \frac{\sin \alpha(Q)}{\alpha(Q)} \, dQ \quad (1)$$

where ρ_0 is the average atomic density and $\alpha(Q) = \pi Q / Q_{max}$.

The local atomic structure of a glass is in many cases similar to that found in at least one crystalline form of the alloy. Thus, the diffraction pattern was calculated for the crystalline low pressure phase GaSb-I and the comparison is presented in Fig. 1. Furthermore, a cluster of hard spheres representing the Ga and Sb atoms in the cubic blende ZnS structure was constructed. The calculated distances in the cluster were compared to the $g(r)$ of the a-GaSb. The agreement with the apparent peaks and shoulders of the experimental curve is rather satisfactory although the peaks are much broader for the amorphous sample.

It should be mentioned in this connection that from the FWHM of the first sharp diffraction peak and the principal peak one can calculate the correlation lengths $\xi_{CC} = 2\pi/\Delta Q_1 = 19$ Å and $\xi_{NN} = 2\pi/\Delta Q_2 = 10$ Å, which values are related to chemical and density fluctuations respectively. The size of the clusters having this local distorted GaSb-I order in a-GaSb is thus, in the range 10–20 Å.

The value of the coordination number of the first nearest neighbors was derived from the $g(r)$. The obtained value is very close to 4 (actually 4.05) which indicates that the structure derives from a compact network with local tetrahedral order (supported by the bond angle $\alpha = 2 \arcsin(r_2/r_1) = 108.6°$, where r_1 and r_2 are distances to nearest and next nearest neighbors, respectively). The nearest neighbor distance, 2.66 Å, in a-GaSb thus turns out to be equal to the sum of the covalent radii of Ga and Sb atoms, 1.26 and 1.40 Å, respectively. This is the r_1 value one thus can expect if, as is the case in the GaSb-I crystal, only unlike atoms are nearest neighbors. The covalent radii of Ga and Sb are noticeably different which means that formation of 'bonds' between like atoms should contribute to an apparent asymmetry in the nearest neighbor separations in a-GaSb. Such an effect is not seen. The FWHM of the first peak is equal to 0.30 Å and it is close to the $\Delta r_1 = 0.278$ Å found in a-Ge [9] by neutron diffraction with similar Q_{max} (23.2 Å^{-1} in [9]). One can therefore conclude that a-GaSb prepared by thermobaric quenching is to a large extent chemically ordered.

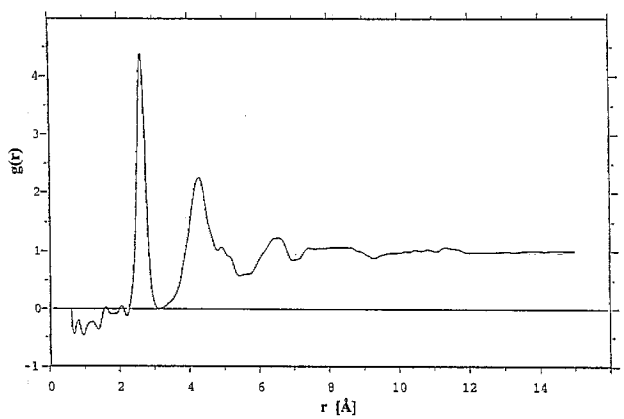

Fig. 2. The total pair distribution function, $g(r)$, for amorphous GaSb obtained by Fourier transformation of $S(Q)$ according to Eq. (1).

The 'relatively perfect structure' (as indicated by the small width of the first peak of $g(r)$) of bulk a-GaSb obtained via the SAMP technique) is rather surprising because the reaction is accompanied by a large volume effect (about 20%) which should result in large internal stresses. The amorphization process also occurs at temperatures well below 300 K where the diffusion ability of the Ga and Sb atoms is low. The high degree of chemical order in a-GaSb produced by the SAMP technique may be due to some kind of order ('memory') remaining from the crystalline phases. In fact, the high pressure phase, GaSb-II, belongs to the so-called 'electronic' phases of Hume–Rothery type [10], which usually show no tendency for chemical ordering. In our experiments, however, this phase was formed from the GaSb-I phase at a moderate temperature and it could hardly have time to reach the equilibrium disordered state. The sample should thus preserve a certain degree of chemical order resulting from the transition GaSb-I to GaSb-II accompanied by a minimum redistribution of atoms through diffusion. On the following amorphization of GaSb-II this order should be favorable for formation of bonds between unlike atoms in a-GaSb which then is expected to have the same type of short-range order as crystalline GaSb-I.

A structural model based on a random packing of ideal tetrahedra to describe the structure of a-GaSb is according to the peak positions in $g(r)$ not completely satisfactory [6]. Furthermore, comparison to the diffraction pattern measured for the crystalline GaSb-I phase explicitly shows that there is, as far as the peak positions are concerned, a close correspondence between the amorphous and the crystalline phases (Fig. 1). It can thus be concluded that the short range order is close to a tetrahedral one but also that the packing of the tetrahedra is made in a distorted continuous network of ZnS blende type.

3.2. ZnSb

Fig. 3 shows the total static structure factor $S(Q)$ for bulk a-$Zn_{41}Sb_{59}$ measured at the SLAD diffractometer. It is obvious that there is a crystalline component in addition to the amorphous one but its magnitude is small and the data are nevertheless useable for a detailed structural analysis. A rough estimation made from the magnitude of the Bragg peaks yields a crystalline concentration less than 0.1%.

From Fig. 3 it is seen that the measured data, contrary to what was the case for a-GaSb, cover a relatively small momentum transfer interval. Thus, the

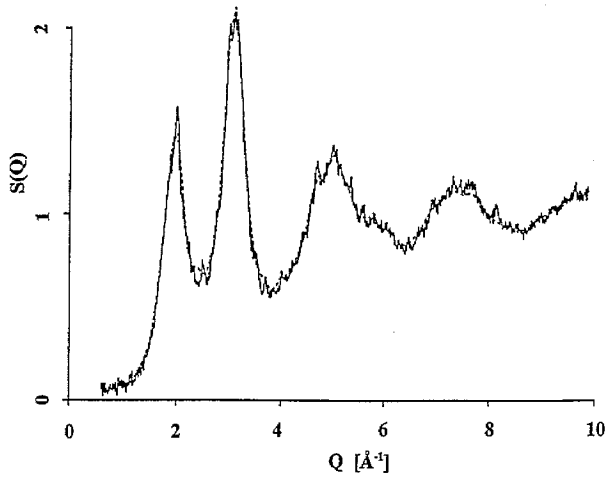

Fig. 3. The structure factor $S(Q)$ for a-$Zn_{41}Sb_{59}$. The solid line represents the experimental data and the broken line the MCGR fit, respectively.

total pair distribution function $g(r)$ was calculated using an inverse method (MCGR). This method works by generating $g(r)$ (without any limitation in r-space) using a Monte Carlo method and then fitting its Fourier transform to the structure factor. A distance of closest approach is, however, introduced as a parameter. Thus the transformation from r-space to Q-space involves no truncation problem of the kind which is usually taken care of by introducing a window function (see above). The resulting $g(r)$ is thus, identically zero below the distance of closest approach. The fit to the $S(Q)$ pattern is shown in Fig. 3 as a broken line. The fitted line coincides with the experimental points within experimental accuracy except where a small contribution from Bragg peaks is observed. The $g(r)$ is given in Fig. 4 and it shows a well defined first peak with an atomic coordination of 4.7 comparable with the coordination of 5 in the equilibrium crystalline structure of ZnSb.

In the crystalline ZnSb, every atom is surrounded by four atoms. One of them is of the same type as the central atom, and the other three are of the second type. A part of the ZnSb unit cell (two interlinked tetrahedra) is presented in Fig. 5. The distances from the central atom to the apices of the tetrahedron are between 2.6 and 2.8 Å. There is also an atom of the second type outside the tetrahedron at the distance from the central atom of about 2.9 Å. Some other interatomic distances are 3.6, 4.0, 4.4, 4.6, 5.1 and 5.3 Å. Thus, the positions of the main peaks of the $g(r)$ curve (Fig. 4) at 2.8, 3.6, 4.2, 4.7 and 5.3 Å could be explained if the short-range order of the atomic arrangement in the amorphous alloy is similar to that in crystalline ZnSb.

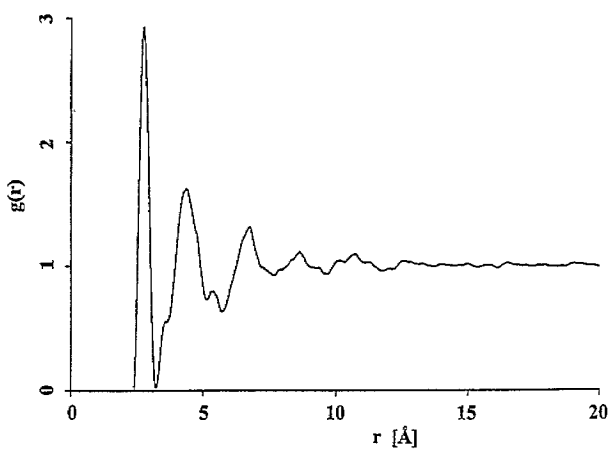

Fig. 4. The total pair distribution function $g(r)$ in a-$Zn_{41}Sb_{59}$ obtained by the MCGR method.

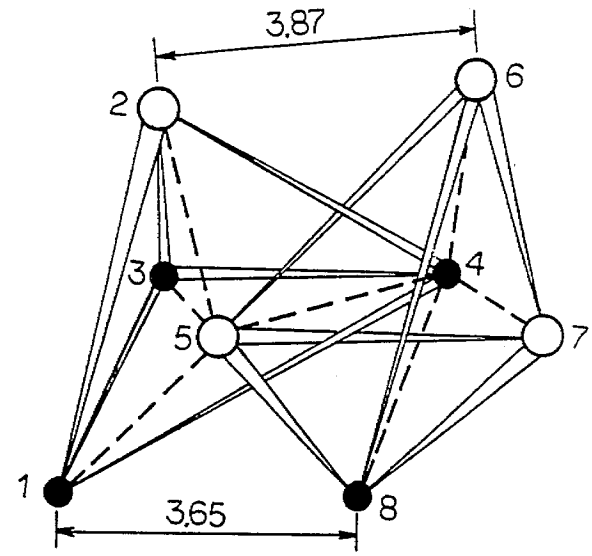

Fig. 5. Local atomic arrangement of the ZnSb crystalline structure [11]. ●, Zn atoms; ○, Sb atoms.

It should be noted that the resolution in r-space of this experiment (because of the small $Q_{max} = 10$ Å^{-1}) was limited to $\Delta r = 2\pi/Q_{max} \approx 0.6$ Å. The analogy with the atomic arrangement in crystalline ZnSb, implies that splitting of the first peak is expected. However, the poor resolution prevents such an observation.

From the results presented above it can be concluded that the atomic local coordination in bulk a-$Zn_{41}Sb_{59}$ is basically tetrahedral. However, the $g(r)$ curve indicates that the tetrahedra are deformed and interlinked in a similar way as is the case in crystalline ZnSb.

4. Comparison with the structure of other amorphous semiconductors and conclusions

The structures of other amorphous materials with tetrahedrally coordinated atoms, germanium [10], silicon [12] and carbon [13] were studied recently by neutron diffraction and analyzed using reverse Monte Carlo (RMC) simulations. A comparative analysis of the structures of amorphous Ge, Si and C based on the

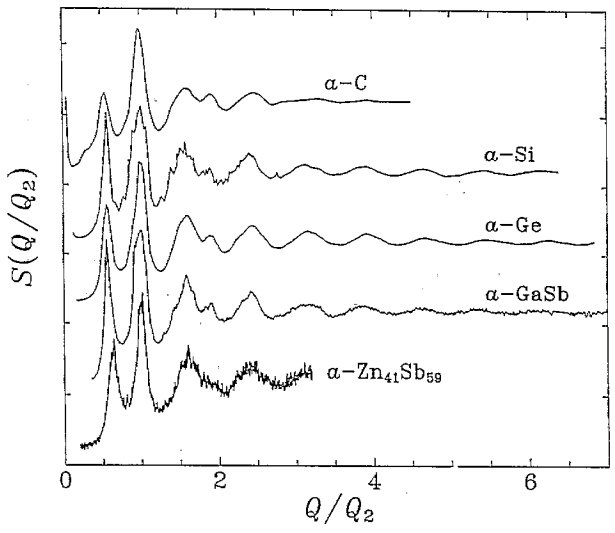

Fig. 6. Experimental structure factors $S(Q/Q_2)$ of amorphous carbon [14], germanium [9], silicon [13], GaSb [6] and $Zn_{41}Sb_{59}$ [5]. Q_2 is the position of second peak in the corresponding $S(Q)$.

results from the RMC simulation has also been carried out in [14]. To eliminate the effect of different atomic radii, to illustrate the construction of the tetrahedral network and to make the comparison of the data for a-$Zn_{41}Sb_{59}$ and a-GaSb with the above-mentioned materials more obvious, the structure factor has been calculated as a function of Q/Q_2, where Q_2 is the position of the second maximum in $S(Q)$. The results are presented in Fig. 6. The choice of the second peak in $S(Q)$ as a reference is motivated by the fact that this is reflecting the concentration dependent atomic fluctuations in a material while the first peak in alloys is due to chemical ordering. The oscillations of $S(Q)$ at Q larger than Q_2 are mainly determined by first and second nearest neighbors distances. As these oscillations are very similar for the different materials it can be concluded that the short-range structure is very similar and in all cases close to tetrahedral. The difference in the packing of the tetrahedra should accordingly manifest itself for $Q/Q_2 < 1.0$.

As is seen from Fig. 6, the $S(Q/Q_2)$ curves differ noticeably in the small Q/Q_2 region which shows that for amorphous materials with tetrahedral bonding the packing of the tetrahedral units is varying from alloy to alloy. In particular, the first sharp diffraction peak in the a-C curve is shifted to the left and that in the a-$Zn_{41}Sb_{59}$ curve to the right as compared to the positions in the other curves. This indicates that the structure of a-C is more open and that the structure of a-$Zn_{41}Sb_{59}$ is more dense than those of the other compounds. The RMC simulations have also shown that the structure of a-Ge and a-Si is well represented by a continuous diamond-like tetrahedral network [14], whereas to successfully model the structure factor of a-C it was necessary to break up such a network (most probably due to the presence of graphite-like defects). In the case of a-$Zn_{41}Sb_{59}$ the tetrahedra of the network were above concluded to be deformed. The similarity between the curves for a-Ge, a-Si and a-GaSb confirms the above proposed structure for a-GaSb as a distorted network of ZnS blende type. The comparison of the structure of different amorphous semiconductors are thus confirming the conclusions drawn above regarding the structure of a-$Zn_{41}Sb_{59}$ and a-GaSb.

Acknowledgements

The work was supported by the Grant No REP300 from the International Science Foundation, by the Russian Government through the Grants No 96-02-18545 (EGP) and 96-02-17486 (OIB) from the Russian Foundation for Fundamental Research and by the Royal Swedish Academy of Sciences under Grant No 1454.

References

[1] E.G. Ponyatovsky and O.I. Barkalov, *Mater. Sci. Rep.*, *8* (1992) 147.
[2] E.G. Ponyatovsky, I.T. Belash and O.I. Barkalov, *J. Non-Cryst. Solids*, *117/118* (1990) 679.
[3] E.G. Ponyatovsky and O.I. Barkalov, *Mater. Sci. Eng.*, *A133* (1991) 726.
[4] V.A. Sidorov, V.V. Brazhkin, L.G. Khvostantsev, A.G. Lyapin, A.V. Sapelkin and O.B. Tsiok, *Phys. Rev. Lett.*, *73* (1993) 3262.
[5] O.I. Barkalov, A.I. Kolesnikov, E.G. Ponyatovsky, U. Dahlborg, R.G. Delaplane and A. Wannberg, *J. Non-Cryst. Solids*, *176* (1994) 263.
[6] M. Calvo-Dahlborg, U. Dahlborg, V.E. Antonov, O.I. Barkalov, A.I. Kolesnikov, E.G. Ponyatovsky and A.C. Hannon, submitted for publication.
[7] V.E. Antonov, A.E. Arakelyan, O.I. Barkalov, A.F. Gurov, E. G. Ponyatovsky, V.I. Rashupkin and V.M. Teplinsky, *J. Alloys Compounds*, *194* (1993) 279.
[8] E.G. Ponyatovsky and T.A. Pozdnyakova, *J. Non-Cryst. Solids*, *188* (1995) 153.
[9] G. Etherington, A.C. Wright, J.T. Wenzel, J.C. Dore, J.H. Clarke and R.N. Sinclair, *J. Non-Cryst. Solids*, *48* (1982) 265.
[10] V.F. Degtyareva and E.G. Ponyatovsky, *Sov. Phys. Solid State*, *24* (1982) 1514.
[11] K. E. Almin, *Acta Chem. Scand.*, *2* (1948) 400.
[12] S. Kugler, L. Pusztai, L. Rosta, P. Chieux and R. Bellissent, *Phys. Rev. B*, *48* (1993) 7685.
[13] K.W.R. Gilkes, P.H. Gaskell and J. Robertson, *Phys. Rev. B*, *51* (1995) 12303.
[14] O. Gereben and L. Pusztai, *Phys. Rev. B*, *50* (1994) 14136.